Metal–Organic Frameworks

Deutsche Ausgabe: DOI: 10.1002/ange.201510084
Internationale Ausgabe: DOI: 10.1002/anie.201510084

Unraveling Inter- and Intrachain Electronics in Polythiophene Assemblies Mediated by Coordination Nanospaces

Michael W. A. MacLean, Takashi Kitao, Takeo Suga, Motohiro Mizuno, Shu Seki, Takashi Uemura, and Susumu Kitagawa**

Abstract: *Strong interchain interactions render unsubstituted polythiophene un-fusible, non-melting, and insoluble. Therefore, control of the packing structure, which has a profound effect on the optical and electronic properties of the polymer, has never been achieved. Unsubstituted polythiophene was prepared in the one-dimensional channels of [La(1,3,5-benzenetrisbenzoate)]$_n$, where polymer chains form unprecedented assembly structures mediated by the host framework. It is noteworthy that the emission and carrier transport properties were drastically changed by varying the number of chains within a particular assembly. The response of the composite to additional guests is also examined as a method to use the composites as low-concentration sensors. Our findings show that the encapsulation of polymer chains in host materials is a facile method for understanding the intrinsic properties of conjugated polymers, along with controlling and enhancing their functions.*

To satisfy a growing global demand for modern electronics, there is an increasing need for flexible materials with emissive and conducting properties. Conjugated polymers have become an interesting way to supplant these needs in organoelectronic and photovoltaic devices.[1] Of particular interest is the heterocyclic variant polythiophene, having garnered much research in the past decades either with attempts to tailor the polymer for high conductivity,[2] or harnessing the semiconducting properties for applications in optical and sensor technologies.[3] One important factor affecting the optical and electronic properties of polythiophene, such as fluorescence and conductivity, is the assembly packing structure of the polymer's local environment. Unsubstituted polythiophene has a longer effective conjugation length than substituted variants due to the lack of perturbation of the backbone planarity that is caused by bulky substituents. This is why unsubstituted polythiophene can be expected to exhibit unique optical and electronic properties through the control of the polymer chain assemblies. Unfortunately, strong interchain interactions render polythiophene un-fusible, non-melting, and insoluble; hence the control of the packing structure, an essential aspect for the discovery of new functions in an established polymer, has never been achieved.

One effective strategy for the control of polymer assemblies involves the use of a porous framework as a host to encapsulate polymer chains.[4] Non-covalent interactions between host and guest, as well as geometrical constraints of the host pores, can induce the formation of new polymer chain assemblies within. These principles have been applied towards the fabrication of single, unsubstituted polythiophene chains within cyclodextrin and zeolite hosts; however, details of the polymer conformation and properties in confined systems such as these remains largely unknown.[5] Furthermore, manipulating the number of polythiophene chains, which is paramount for the optical and electronic properties, has remained a major challenge.

Porous coordination polymers (PCPs) or metal–organic frameworks (MOFs), prepared by the self-assembly of metal ions and functional ligands, are currently under investigation for a variety of potential applications including, but not limited to, gas storage and separation, ion conductivity, and heterogeneous catalysis.[6] The characteristic features of PCPs are their highly regular and controllable channels that vary in accordance with the metal ions and organic linkers used. It is these advantages that allow us to achieve precise polymer assemblies within the regular nanochannels of PCPs, and can be expected to have great benefits, not only to answer fundamental questions about the nature of the discrete polymer, but also offering the potential to create polymers with optimized functions.[7]

Herein, we report the effective encapsulation, isolation, and systematic amalgamation of unsubstituted polythiophene

[*] M. W. A. MacLean
Department of Chemistry, Queen's University
90 Bader Lane, Kingston, Ontario, K7L 3N6 (Canada)
T. Kitao, Dr. T. Uemura, Prof. S. Kitagawa
Department of Synthetic Chemistry and Biological Chemistry
Graduate School of Engineering, Kyoto University
Katsura, Nishikyo-ku, Kyoto 615-8510 (Japan)
E-mail: uemura@sbchem.kyoto-u.ac.jp
kitagawa@icems.kyoto-u.ac.jp
Dr. T. Suga
Department of Applied Chemistry, Waseda University
3-4-1 Ohkubo, Shinjuku, Tokyo 169-8555 (Japan)
Prof. Dr. M. Mizuno
Department of Chemistry, Graduate School of Natural Science & Technology, Kanazawa University
Kakuma, Kanazawa, Ishikawa 920-1192 (Japan)
Prof. Dr. S. Seki
Department of Molecular Engineering
Graduate School of Engineering, Kyoto University
Katsura, Nishikyo-ku, Kyoto 615-8510 (Japan)
Dr. T. Uemura
CREST Japan Science and Technology Agency (JST)
4-1-8 Honcho, Kawaguchi, Saitama 332-0012 (Japan)
Prof. S. Kitagawa
Institute for Integrated Cell-Material Sciences (iCeMS)
Kyoto University, Yoshida, Sakyo-ku, Kyoto 606-8501 (Japan)

Supporting information for this article is available on the WWW under http://dx.doi.org/10.1002/anie.201510084.

to form unprecedented assembly structures that exhibit unique fluorescence and conducting behaviors. By varying the number of chains within a particular assembly, the aforementioned properties were drastically changed, a feat that was unbeknownst for such systems. As conjugated polymers were designed to serve as molecular wires and emitting elements in advanced nanoscale devices,[8] future applications will require a deeper understanding of nanoscale electronics that can only be realized through the unraveling of the optical and electrical properties in low dimensional polymer assemblies that, until now, have remained elusive. The obtained results indicate that our method is a significant approach, not only for enhancing and controlling the functions of unprocessable polymers, but also for broadening the understanding the true nature of conjugated polymers.

The synthesis of the polymer–PCP composites is illustrated in Scheme 1. First, the vapor adsorption of the monomer (2,2′:5′,2″-terthiophene, TTh) throughout the internal and external surface of the PCP $[La(BTB)]_n$ (**1**; BTB = 1,3,5-benzentrisbenzoate), which has one-dimensional regular nanopores along the *c*-axis (channel size = 10.7 × 10.7 Å^2);[9] then, the externally adsorbed monomer was removed to ensure an even distribution of monomer throughout the channels of the host;[10] and finally, the polymerization was achieved by a similar vapor adsorption of iodine throughout the host–TTh composite followed by heating at 90 °C for 12 h to perform the oxidative polymerization of TTh within the channels of the host and afford the PCP-unsubstituted polythiophene composite (**1**⊃PTh). To control the assembly state of PTh, the weight ratio between TTh and **1** was systematically increased (**1**⊃PTh·*x*; where *x* represents the weight ratio of PTh to **1**⊃PTh). Oxidative polymerization of TTh results in p-doped PTh, which exhibits different absorption properties and must be converted into the undoped state by treatment with a mild reductant, in this case dilute hydrazine. The UV/Vis spectra of **1**⊃PTh indicated that PTh confined in **1** was in the neutral state (Supporting Information, Figure S1).[11] In fact, I_2 was not detected in Scanning electron microscopy-energy dispersive X-ray (SEM-EDX) measurements of **1**⊃PTh after the dedoping treatment (Supporting Information, Figure S2). The amount of I_2 in the composite was negligible (< 1 wt %), which was shown by X-ray fluorescence spectroscopy. Powder X-ray diffraction (PXRD) measurements of **1**⊃PTh indicated that the channel structure of **1** was maintained during the polymerization and dedoping processes (Supporting Information, Figure S3). The obvious changes in the relative intensities in the PXRD pattern were detected after the polymerization in **1**, which was ascribed to the change of electron density in the pores.[7c,12] SEM-EDX elemental mapping measurements confirmed the homogeneous distribution of polymer chains in the channels of **1** through the homogeneous dispersion of S atoms in the PCP crystals (Supporting Information, Figure S4). The particle size distribution of **1**⊃PTh was almost the same to that of the original host, indicating no PTh existed outside **1** (Supporting Information, Figure S5). Furthermore, the adsorption isotherms of **1**⊃PTh exhibited a drastic decrease in the amount of adsorption compared with those of **1** (Supporting Information, Figure S6). All these results clearly indicated the accommodation of PTh in the nanochannels of **1**. PTh from composites prepared in this manner could be more thoroughly analyzed once they were liberated from the host using an aqueous solution of sodium ethylenediaminetetraacetate. MALDI-TOF-MS, solid-state ^{13}C NMR, and PXRD measurements showed the typical characteristics of PTh devoid of branching (maximum molecular weight = 2700; Supporting Information, Figures S3, S7, and S8); and the conversion from Th into PTh was over 90 % (determined by isolated yield).[11c] In SEM measurements, it is of interest that the morphology of the recovered PTh objects retained the microrod shape of the original host (Supporting Information, Figure S9). This is a clear demonstration that polymerization occurs entirely within the crystalline framework.[4a]

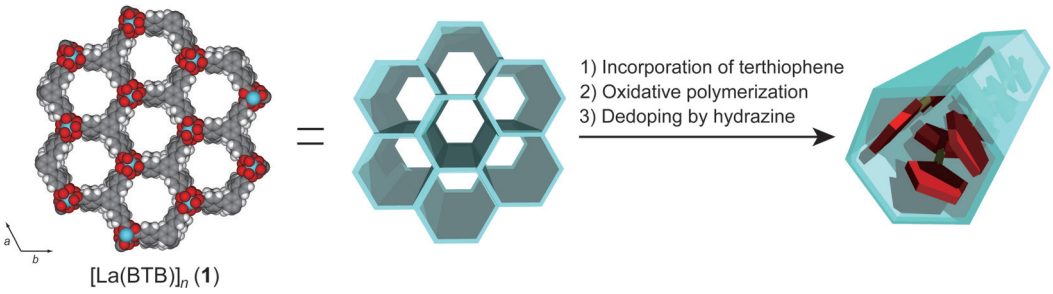

Scheme 1. Synthetic strategy for the confinement of unsubstituted polythiophene (PTh) within the 1D channels of **1**.

Initial studies, aiming to explore the local conformation of the PTh confined within the nanopores, were facilitated using Raman spectroscopy, where the intensity of the PTh within the pores was selectively enhanced through resonance Raman effects with incident laser frequency of 785 nm. The Raman spectra of **1**⊃PTh·30 (Figure 1 a; Supporting Information, Figure S10) shows the C=C in-phase stretching mode at 1454 cm^{-1}, suggesting that the backbone exists in a planar confirmation.[13] The peak shift of the C=C in-phase stretching mode, and therefore the planarity, is fairly independent of the amount of PTh in **1**, and is even maintained in composites containing only small amounts of PTh (**1**⊃PTh·5).

Molecular scale motion of polymers has been heavily explored through ^{2}H NMR studies on deuterated analogues. To probe the molecular motion of polythiophene within **1**⊃PTh, we prepared the 3,4,5,3′,4′,3″,4″,5″-octadeutero-2,2′:5′:2″-terthiophene (DTh) and polymerized it within the pores of **1** in a similar fashion to give **1**⊃PDTh·5 and **1**⊃PDTh·30. The ^{2}H NMR spectra of **1**⊃PDTh (Figure 1 b) showed typical rigid limit line shape indicating that the

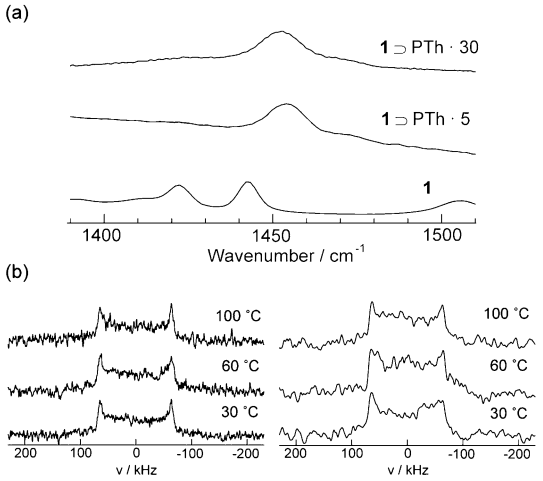

Figure 1. a) Raman spectra of **1**⊃PTh. b) ^{2}H NMR spectra of **1**⊃PDTH·*x* (*x* = weight ratio of DPTh to **1**⊃PDTh). *x* = 30 (left) and *x* = 5 (right).

exchange of chemical environments is ultraslow regardless of temperature and loading amount. This provides further support that the polymer chains exist statically in **1** without rotation of the thiophene rings.

The specific assembly of the PTh chains confined in **1** should play a crucial role for the optical and electronic properties; hence, they were studied using molecular dynamics (MD) simulations (Figure 2). The conformation of the

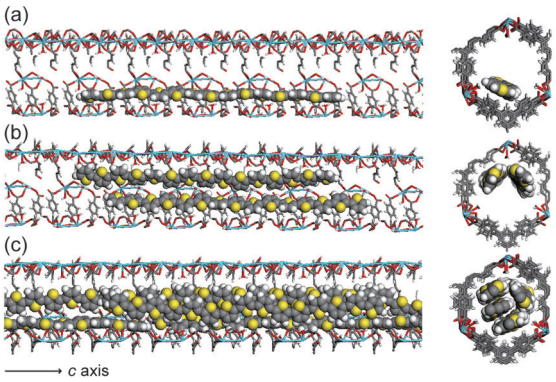

Figure 2. MD structures of the PTh chain assemblies confined in the nanochannels of **1**: a) **1**⊃PTh·6, b) **1**⊃PTh·15, and c) **1**⊃PTh·30. S yellow, La light blue, O red, C gray, H white.

confined PTh seems almost planar, which is fairly consistent with the results of Raman and ^{2}H NMR spectroscopy measurements. This holds true even for systems with low PTh loading, despite the low torsional energy barrier that is expected to exist between the two thiophene rings (3.5 kcal mol^{-1} for the isolated polythiophene).[14] The lack of twisting can be explained by the association of the polymer with the walls of the host, as observed through the presences of CH···π interactions in the MD simulation. It is these interactions that are suspected to be responsible for increasing the energy barrier enough to inhibit rotation about the backbone,[15] as confirmed by ^{2}H NMR measurements.

By controlling the amount of TTh present during the vapor adsorption, we are able to give rise to a variety of different sized polythiophene assemblies. MD simulations indicated that the monochain and dichain (assemblies of two polymer chains) exist in the composites with lower PTh loading, whereas trichain and tetrachain assemblies are formed as the loading of PTh is increased. Regardless of the number of chains within a given pore, the PTh chains exist in a planar fashion with no evidence of twisting. Furthermore, it is striking that the confined PTh chain assemblies in **1**⊃PTh·30 formed cofacial π-stacked structure, which is completely different from the herringbone packing that is observed in the bulk state.[16]

To investigate the optical properties of chain assemblies mediated by **1** we carried out fluorescence measurements of the **1**⊃PTh composites (Figure 3a; Supporting Information,

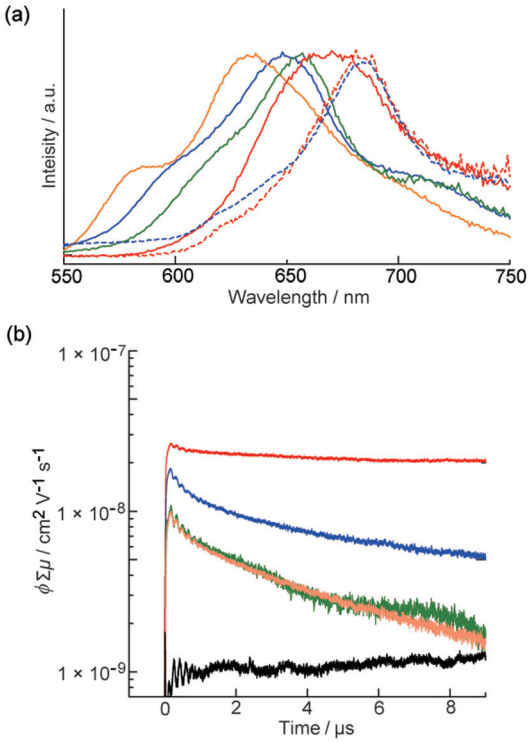

Figure 3. a) Fluorescence spectra (excitation at 468 nm) for **1**⊃PTh·22 (red line), **1**⊃PTh·15 (green), **1**⊃PTh·5 (blue), **1**⊃PTh·5 after exposure to MeOH (orange); as well as liberated PTh from **1**⊃PTh·22 (red dashed line) and **1**⊃PTh·5 (blue dashed line). b) Kinetics traces of conductivity transients observed for **1** (black), **1**⊃PTh·5 (orange), **1**⊃PTh·15 (green), **1**⊃PTh·22 (blue), and **1**⊃PTh·30 (red) upon exposure to 355 nm pulses at 7.7–8.9×10^{15} photons cm^{-2}. Transients were recorded at RT under O_2 saturated atmosphere.

Figure S11). Accommodation of PTh chains in **1** resulted in a blue-shift of the emission wavelength in all cases; moreover, as the loading of the polymer within the channels is decreased, the magnitude of the blue-shift is increased (**1**⊃PTh·22 670 nm, **1**⊃PTh·5 647 nm).[17] Aggregated polythiophenes, in which the excitons can migrate among neighboring chains to reach the lowest-energy sites, show a red-shifted emission peak with respect to the isolated chains

(as was observed upon the dissolution of the host framework; Figure 3a, dashed lines).[18] MD simulations suggested that polymer assemblies containing fewer chains are formed as the composite loading is decreased; therefore, the largest blue-shifted emission of **1**⊃PTh·5 would be attributed to the greatest chance of finding a discrete polymer chain within the channels of the PCP.

Along with changes in the energy of the emission caused by encapsulation, the quantum efficiencies were affected by entrapment of the polymer within the PCP framework. The highest quantum efficiency (2%) can be seen for **1**⊃PTh·5 while **1**⊃PTh·22 and bulk polymer had quantum efficiencies of 0.5% and 0.2%, respectively.

These obtained results illustrate that the accommodation of polymer chains within host materials is a key strategy for modulating and enhancing the luminescence of unprocessable polymers. Moreover, this method provides an opportunity for the development of sensing devices because the extra space within the host pores can further accommodate additional molecules (for example, gas and solvents). The new guests should affect the polymer assembly structures to bring about changes in the optical and electronic properties of the polymer, a phenomenon that is less prevalent for bulk PTh owing to strong interchain aggregation. For example, although the emission peak of bulk PTh was not changed before and after the addition of MeOH (Supporting Information, Figure S12), a large blue-shift is observed when the PTh composites were subjected to MeOH vapor (Figure 3a). These shifts are most prominent for **1**⊃PTh·5 due to the larger sized void available for the diffusion of MeOH molecules. Although the blue-shifting of the emission of polythiophene upon exposure to methanol is contradictory to what is observed for bulk PTh, it can be rationalized by the coordination of MeOH molecules to the open metal sites of **1**, a phenomenon that is confirmed by single crystal analysis in analogous systems.[9] In fact, other vapor molecules without hydroxy functionality do not induce a large emission shift for PTh in **1** (Supporting Information, Figure S13). The coordination of MeOH molecules to the open metal sites of **1** would inhibit the CH···π interaction between PTh and **1** to cause the perturbation of the backbone planarity and, in turn, decreases the effective conjugation length to result in a blue-shift of the emission. Raman spectra of **1**⊃PTh·5 upon exposure to MeOH vapor shows a shift in the band at 1454 cm^{-1} to longer wavenumber, and can be attributed to a loss of planarity of the backbone (Supporting Information, Figure S14).[19] As the adsorption isotherm of MeOH for **1**⊃PTh·5 shows a steep rise even in the low-pressure region, it demonstrates that the hybridization of functional polymers within porous materials is a key strategy for sensing systems intended to detect very low concentration of vapors (Supporting Information, Figure S15).

The carrier transporting properties of conducting polymers confined in the pores cannot be evaluated appropriately by bulk conductivity measurements, such as time-of-flight, because the polymer chain assemblies are decoupled from each other in the pores (Supporting Information, Figure S16).[4f] In contrast, flash-photolysis time-resolved microwave conductivity (FP-TRMC) measurement enables intrinsic charge carrier mobility of the polymers to be evaluated even in the pores because TRMC is not influenced by the connectivity between the polymer assemblies.[20] Thus, TRMC was employed to study the carrier transport properties of the PTh chain assemblies contained within **1**. Upon exposure of composite **1**⊃PTh to a laser pulse with excitation wavelength of 355 nm, a rapid rise of the transient conductivity ($\phi\Sigma\mu$, where ϕ and $\Sigma\mu$ are the charge carrier generation yield and the sum of the charge carrier mobilities, respectively) was observed (Figure 3b). Conversely, the transient conductivity profile for the unoccupied host showed no such rapid increase, thus confirming that the conductivity signal observed in **1**⊃PTh is a result of the guest PTh rather than the host **1**. The value of μ in **1**⊃PTh was calculated on the basis of $\phi\Sigma\mu$ and ϕ, which could be derived from TRMC and transient absorption measurements, respectively (Supporting Information, Figures S17 and S18). It is also worthy to note that a discontinuous change in the carrier mobility of PTh was observed as the amount of polymer chains was increased. For example, when the loading of PTh within **1**⊃PTh was small, the carrier mobility of PTh remained unchanged ($\mu = 0.04\ cm^2 V^{-1} s^{-1}$) until the PTh loading reaches approximately 15% w/w. After this threshold, the carrier mobility is rapidly increased to a maximum mobility of $0.3\ cm^2 V^{-1} s^{-1}$ in **1**⊃PTh·30. It has been proposed that the key factor in effective carrier transport is π-orbital overlap, which is also responsible for dictating the inter-chain orientations in PTh.[21] As the MD simulations of **1**⊃PTh have suggested, the assembly structure of PTh confined in **1** is varied and depends largely on the amount of PTh within the host; an increase in the amount of PTh would lead to the formation of unique cofacial π-stacking structure within the assemblies, and this is to be attributed to the enhanced charge carrier mobility. Furthermore, it should be noted that the hole mobility of **1**⊃PTh·30 exhibited a very low decay rate constant when compared with the lower loaded **1**⊃PTh analogues. This suggests that the π-stacked aggregation of the polymer prevents the holes from undergoing a charge recombination process.

The local motion of charge carriers in a particular assembly, induced by the electric field of the probing microwave when operated in alternating current mode, is dependent on the thermal diffusive motion of the polymer within the time constant (τ) of the cavity employed ($\tau \approx 100$ ns within the cavity with a Q factor of about 10^3 for the probing microwave frequency $f \approx 9 \times 10^9\ s^{-1}$). Here, the conjugated backbone of PTh, as well as the cofacial polymer aggregates serves as a platform for the positive holes to diffuse about the polymer when confined in **1**. The following Kubo equation derived from Einstein–Smoluchowski relation provides an estimate of spatial size (Δx) of the statistical local motion of holes within the assemblies [Eq. (1); where k_B and e are Boltzmann's constant and the elementary charge, respectively].[22]

$$\Delta x = (\mu k_B T f^{-1} e^{-1})^{1/2} \quad (1)$$

The value of Δx, and thereby an estimate of the effective conjugation length, was 3.2 nm in **1**⊃PTh·5; this is comparable

with reported values of averaged conjugation length in single polythiophene chains,[23] while Δx value in **1**⊃PTh·30 was found to be 8.8 nm. These results suggest that the controlled packing of the polymer chains plays a remarkable role in extending the conjugation of the system without any change in chemical composition of the components.

The carrier transport behavior of PTh in low-dimensional assemblies, containing few chains of polymer, has been unknown owing to the lack of effective methods for the manipulation of individual chains. By utilizing regular PCP channels as host matrices, we have succeeded in controlling the number of polymer chains for the first time and, in doing so, have shed light on the discontinuous relationship between the number of polymer chains and the carrier transport properties through the formation of a π–π stacked structure. This provides a deeper understanding for future design and optimization of molecular-scale devices.

In conclusion, we have demonstrated a simple and effective method for the control and enhancement of the optical and electronic properties of polythiophene, a promising heterocyclic conjugated polymer that is not amenable to processing by traditional means, through the use of a microporous PCP host. The obtained results illustrate that encapsulation of polymer chains is a key strategy to control the chain assembly structures with precision. In this regard, numerous other unprocessable polymers, such as unsubstituted polyfluorene and poly(*p*-phenylene vinylene), can be controlled in a similar fashion to elicit potentially useful yet unexplored properties. We believe that these findings will contribute not only to the preparation of a variety of advanced nanocomposite materials based on PCPs and functional polymers but also significantly towards the understanding of the intrinsic properties of conjugated polymers in general.

Acknowledgements

This work was supported by the JST, CREST program, and a Grant-in Aid for Science Reserch on Innovative Area "New Polymeric Materials Based on Element-Blocks (No. 2401) from the Ministry of Education, Culture, Sports, Science and Technology, Government of Japan. M.W.A.M. thanks the government of Ontario and Queen's University for Scholarships; NSERC's CREATE program and Queen's SGS for funding his research abroad; and Prof C. M. Crudden for brokering this research exchange.

Keywords: conjugated polymers · host–guest systems · metal–organic frameworks · microporous materials · polymerization

How to cite: *Angew. Chem. Int. Ed.* **2016**, *55*, 708–713
Angew. Chem. **2016**, *128*, 718–723

[1] a) J. Janata, M. Josowicz, *Nat. Mater.* **2003**, *2*, 19–24; b) A. J. Heeger, *Chem. Soc. Rev.* **2010**, *39*, 2354–2371.

[2] a) J. Roncali, *Chem. Rev.* **1992**, *92*, 711–738; b) T. Yamamoto, A. Morita, Y. Miyazaki, T. Maruyama, H. Wakayama, Z. H. Zhou, Y. Nakamura, T. Kanbara, S. Sasaki, K. Kubota, *Macromolecules* **1992**, *25*, 1214–1223.

[3] a) A. Mishra, C.-Q. Ma, P. Bäuerle, *Chem. Rev.* **2009**, *109*, 1141–1276; b) S. Nejati, T. E. Minford, Y. Y. Smolin, K. K. S. Lau, *ACS Nano* **2014**, *8*, 5413–5422; c) B. A. G. Hammer, M. A. Reyes-Martinez, F. A. Bokel, F. Liu, T. P. Russell, R. C. Hayward, A. L. Briseno, T. Emrick, *ACS Appl. Mater. Interfaces* **2014**, *6*, 7705–7711; d) C. Li, G. Shi, *ACS Appl. Mater. Interfaces* **2013**, *5*, 4503–4510; e) V. C. Gonçalves, D. T. Balogh, *Sens. Actuators B* **2012**, *162*, 307–312.

[4] a) P. Sozzani, S. Bracco, A. Comotti, P. Valsesia, R. Simonutti, O. Terasaki, Y. Sakamoto, *Nat. Mater.* **2006**, *5*, 545–551; b) G. Distefano, A. Comotti, S. Bracco, M. Beretta, P. Sozzani, *Angew. Chem. Int. Ed.* **2012**, *51*, 9258–9262; *Angew. Chem.* **2012**, *124*, 9392–9396; c) P. Sozzani, A. Comotti, S. Bracco, R. Simonutti, *Angew. Chem. Int. Ed.* **2004**, *43*, 2792–2797; *Angew. Chem.* **2004**, *116*, 2852–2857; d) T.-Q. Nguyen, J. Wu, V. Doan, B. J. Schwartz, S. H. Tolbert, *Science* **2000**, *288*, 652–656; e) A. Comotti, S. Bracco, M. Mauri, S. Mottadelli, T. Ben, S. Qiu, P. Sozzani, *Angew. Chem. Int. Ed.* **2012**, *51*, 10136–10140; *Angew. Chem.* **2012**, *124*, 10283–10287; f) C.-G. Wu, T. Bein, *Science* **1994**, *264*, 1757–1759; g) S. Esnouf, F. Beuneu, P. Enzel, T. Bein, *Phys. Rev. B* **1997**, *56*, 12899–12904; h) F. Cucinotta, F. Carniato, G. Paul, S. Bracco, C. Bisio, S. Caldarelli, L. Marchese, *Chem. Mater.* **2011**, *23*, 2803–2809; i) J. Gierschner, L. Lüer, D. Oelkrug, E. Musluoğlu, B. Behnisch, M. Hanack, *Adv. Mater.* **2000**, *12*, 757–761; j) D. J. Cardin, *Adv. Mater.* **2002**, *14*, 553–563; k) E. Aharon, M. Kalina, G. L. Frey, *J. Am. Chem. Soc.* **2006**, *128*, 15968–15969; l) E. Aharon, A. Albo, M. Kalina, G. L. Frey, *Adv. Funct. Mater.* **2006**, *16*, 980–986; m) Y. Honmou, S. Hirata, H. Komiyama, J. Hiyoshi, S. Kawauchi, T. Iyoda, M. Vacha, *Nat. Commun.* **2014**, *5*, 4666; n) M. S. Cho, H. J. Choi, W. S. Ahn, *Langmuir* **2004**, *20*, 202–207.

[5] a) M. van den Boogaard, G. Bonnet, P. van't Hof, Y. Wang, C. Brochon, P. van Hutten, A. Lapp, G. Hadziioannou, *Chem. Mater.* **2004**, *16*, 4383–4385; b) P. Enzel, T. Bein, *J. Chem. Soc. Chem. Commun.* **1989**, 1326–1327.

[6] a) O. M. Yaghi, M. O'Keeffe, N. W. Ockwig, H. K. Chae, M. Eddaoudi, J. Kim, *Nature* **2003**, *423*, 705–714; b) G. Férey, *Chem. Soc. Rev.* **2008**, *37*, 191–214; c) S. Kitagawa, R. Kitaura, S.-i. Noro, *Angew. Chem. Int. Ed.* **2004**, *43*, 2334–2375; *Angew. Chem.* **2004**, *116*, 2388–2430; d) P. Ramaswamy, N. E. Wong, G. K. H. Shimizu, *Chem. Soc. Rev.* **2014**, *43*, 5913–5932.

[7] a) T. Uemura, K. Kitagawa, S. Horike, T. Kawamura, S. Kitagawa, *Chem. Commun.* **2005**, 5968–5970; b) T. Uemura, N. Yanai, S. Watanabe, H. Tanaka, R. Numaguchi, M. T. Miyahara, Y. Ohta, M. Nagaoka, S. Kitagawa, *Nat. Commun.* **2010**, *1*, 83; c) T. Uemura, N. Uchida, A. Asano, A. Saeki, S. Seki, M. Tsujimoto, S. Isoda, S. Kitagawa, *J. Am. Chem. Soc.* **2012**, *134*, 8360–8363; d) G. Distefano, H. Suzuki, M. Tsujimoto, S. Isoda, S. Bracco, A. Comotti, P. Sozzani, T. Uemura, S. Kitagawa, *Nat. Chem.* **2013**, *5*, 335–341.

[8] a) R. M. Metzger, *Chem. Rev.* **2003**, *103*, 3803–3834; b) G. Reecht, F. Scheurer, V. Speisser, Y. J. Dappe, F. Mathevet, G. Schull, *Phys. Rev. Lett.* **2014**, *112*, 047403.

[9] a) T. Devic, C. Serre, N. Audebrand, J. Marrot, G. Férey, *J. Am. Chem. Soc.* **2005**, *127*, 12788–12789; b) J. Duan, M. Higuchi, S. Horike, M. L. Foo, K. P. Rao, Y. Inubushi, T. Fukushima, S. Kitagawa, *Adv. Funct. Mater.* **2013**, *23*, 3525–3530.

[10] This was confirmed through XRPD data (Supporting Information, Figure S3) owing to the lack of peaks corresponding to TTh, indicating that all of the TTh must be present within the pores.

[11] a) K. Kaneko, S. Hayashi, S. Ura, K. Yoshino, *J. Phys. Soc. Jpn.* **1985**, *54*, 1146–1153; b) D. Ofer, R. M. Crooks, M. S. Wrighton, *J. Am. Chem. Soc.* **1990**, *112*, 7869–7879; c) J. Chen, J. Shu, S. Schobloch, A. Kroeger, R. Graf, R. Muñoz-Espí, K. Landfester, U. Ziener, *Macromolecules* **2012**, *45*, 5108–5113.

[12] B. Marler, U. Oberhagemann, S. Vortmann, H. Gies, *Microporous Mater.* **1996**, *6*, 375–383.

[13] a) E. M. Bazzaoui, J. P. Marsault, S. Aeiyach, P. C. Lacaze, *Synth. Met.* **1994**, *66*, 217 – 224; b) S. Garreau, M. Leclerc, N. Errien, G. Louarn, *Macromolecules* **2003**, *36*, 692 – 697.
[14] E. C. Vujanovich, J. W. G. Bloom, S. E. Wheeler, *J. Phys. Chem. A* **2012**, *116*, 2997 – 3003.
[15] H. Yamashita, T. Yumura, *J. Phys. Chem. C* **2012**, *116*, 9681 – 9690.
[16] S. Brückner, W. Porzio, *Makromol. Chem.* **1988**, *189*, 961 – 967.
[17] **1**⊃PTh·30 showed the emission peak around 680 nm; however, it was very weak (quantum yield < 0.1 %), probably because of the concentration self-quenching (Supporting Information, Figure S11).
[18] a) J. J. Apperloo, R. A. J. Janssen, P. R. L. Malenfant, J. M. J. Fréchet, *Macromolecules* **2000**, *33*, 7038 – 7043; b) T. Fukuda, Y. Inoue, T. Koga, M. Matsuoka, Y. Miura, *Chem. Lett.* **2011**, *40*, 864 – 866; c) A. Ruseckas, E. B. Namdas, M. Theander, M. Svensson, A. Yartsev, D. Zigmantas, M. R. Andersson, O. Inganäs, V. Sundström, *J. Photochem. Photobiol. A* **2001**, *144*, 3 – 12.
[19] Y. Noguchi, A. Saeki, T. Fujiwara, S. Yamanaka, M. Kumano, T. Sakurai, N. Matsuyama, M. Nakano, N. Hirao, Y. Ohishi, S. Seki, *J. Phys. Chem. B* **2015**, *119*, 7219 – 7230.
[20] a) A. Saeki, S. Seki, T. Sunagawa, K. Ushida, S. Tagawa, *Philos. Mag.* **2006**, *86*, 1261 – 1276; b) A. Saeki, S. Seki, Y. Koizumi, T. Sunagawa, K. Ushida, S. Tagawa, *J. Phys. Chem. B* **2005**, *109*, 10015 – 10019.
[21] G. R. Hutchison, M. A. Ratner, T. J. Marks, *J. Am. Chem. Soc.* **2005**, *127*, 16866 – 16881.
[22] a) R. Kubo, *Rep. Prog. Phys.* **1966**, *29*, 255 – 284; b) R. Kubo, *J. Phys. Soc. Jpn.* **1957**, *12*, 570 – 586.
[23] a) N. Takeda, J. R. Miller, *J. Phys. Chem. B* **2012**, *116*, 14715 – 14723; b) H. Meier, U. Stalmach, H. Kolshorn, *Acta Polym.* **1997**, *48*, 379 – 384.

Received: October 29, 2015
Published online: November 26, 2015

